

Nature of the hole states in Li-doped NiO

Hungru Chen and John H. Harding

Department of Materials Science and Engineering, University of Sheffield, S1 3JD, United Kingdom

(Received 7 November 2011; revised manuscript received 23 February 2012; published 28 March 2012)

We have performed density functional calculations on $\text{Li}_{0.125}\text{Ni}_{0.875}\text{O}$ using both the HSE06 hybrid functional and the density functional theory (DFT) + U method. Contrary to previous calculations, both methods show that the system is better described with the hole localized on the nickel ion (which is thus formally Ni^{3+}) rather than in the oxygen valence band. We discuss the experimental results in the light of this finding and show that it is consistent with the available data.

DOI: [10.1103/PhysRevB.85.115127](https://doi.org/10.1103/PhysRevB.85.115127)

PACS number(s): 71.15.Mb

I. INTRODUCTION

Hole-doped Mott insulators have attracted considerable attention due to the discovery of high-temperature superconducting cuprates. One basic question is the nature of the hole state in Mott-insulating systems. NiO is traditionally considered to be a prototype Mott insulator with a wide band gap. It is often classified as a charge-transfer insulator, although the original Zaanen-Sawatzky-Allen paper¹ suggested that it is on the borderline between a charge-transfer and a Mott-Hubbard insulator. Indeed, recent work suggests a mixture of charge-transfer and Mott-Hubbard character,² although most experimental and theoretical work has apparently supported the charge-transfer nature of the band gap in NiO.^{3–6} Hole doping in NiO is usually obtained by doping NiO with lithium oxide (with which it forms an extensive solid solution) whereby Ni^{2+} is replaced by Li^+ . Antolini⁷ has summarized the experimental evidence on the question of the nature of the hole. The older magnetic measurement studies adopted Ni^{3+} as the relevant nickel charge state for interpreting their results,⁸ as do all the current studies on the related compound LiNiO_2 .⁹ Changes in the Ni-Ni bond length with the composition x of $\text{Li}_x\text{Ni}_{1-x}\text{O}$ obtained from nickel K -edge x-ray-absorption fine-structure spectroscopy¹⁰ support the idea that the nickel ion should be considered as Ni^{3+} —i.e., the hole is on the metal. On the other hand, oxygen K -edge x-ray-absorption spectroscopy of $\text{Li}_x\text{Ni}_{1-x}\text{O}$ has been interpreted in terms of holes on the oxygen atoms.¹¹ This interpretation relies on ideas taken from an analysis of excitations in pure NiO.³ This work, together with a number of *ab initio* calculations^{12,13} discussed below, is the justification of the idea that the hole is in the oxygen valence band, localized on an oxide ion next to the Li dopant (hence formally producing an O^- ion).

Previous theoretical work using spin-unrestricted Hartree-Fock and hybrid functionals with a high percentage of Fock exchange predicted that the hole states resided mainly on oxygen.^{12,13} However, the high percentages of Fock exchange used lead to an unreasonably large band gap in NiO;^{14,15} in effect these methods overemphasize an ionic description. Consequently the valence-band edge was found to consist exclusively of oxygen states in these calculations. This is not consistent with the large contribution from Ni states seen in the valence-band edge in experiment.³ Recent work using dynamic-mean-field theory (DMFT) calculations also

predicted oxygen holes.¹⁶ However, that calculation ignores the Li ion completely except for its ability to generate holes. This discounts both the structure relaxation and the Li impurity potential. Moreover, these calculations failed to reproduce the “surviving” gap upon Li doping observed in oxygen K -edge x-ray-absorption spectra which the previous authors¹⁰ ascribed to a localizing potential. We have therefore performed calculations that explicitly include the Li ion, performed within periodic boundary conditions rather than using a finite cluster.

II. METHOD

In this study, we investigate the electronic structure of Li-doped NiO by hybrid functional first-principles density functional theory calculations, with the projector augmented wave approach.¹⁷ The HSE06 hybrid functional, which mixes 25% of Hartree-Fock exchange with 75% of the Perdew-Burke-Ernzerhof functional, is used.¹⁸ The inclusion of Hartree-Fock exchange corrects the self-interaction error contained in standard density functional theory (DFT) functionals and so greatly improves the description of strongly correlated systems such as transition-metal oxides. It has been shown previously that 20%–35% of exact exchange in DFT calculations results in good physical properties for NiO.¹⁴

An alternative method of treating strongly correlated systems is to include an on-site Coulomb interaction, the Hubbard U parameter, in the standard DFT calculations. This is known as the DFT + U method. Calculations using this method were also performed to compare with the HSE06 results. The rotational invariant form¹⁹ of the DFT + U formalism was used and $U_{\text{eff}} = U - J$, the on-site correction, was set to be 5.3 eV for Ni $3d$ electrons. The number is taken from a previous study on NiO in which this U_{eff} value was shown to give reasonable physical properties.²⁰ To model Li-doped NiO, we consider a single composition whereby one Ni is replaced by Li in a $2 \times 2 \times 2$ antiferromagnetic NiO supercell with eight formula units. This corresponds to a nonstoichiometry of $x = 0.125$ in $\text{Li}_x\text{Ni}_{1-x}\text{O}$, which is well within the experimental range^{10,11} and, moreover, was the composition chosen for the Hartree-Fock calculations discussed above.^{12,13} The computational requirements of using the HSE06 functional preclude a full study across a range of compositions, but this one composition is sufficient for

TABLE I. Comparison of calculated and experimentally measured properties of NiO.

	Lattice parameter (Å)	Ni magnetic moment (μ_B)	Band gap (eV)
HSE06	4.179	1.66	4.1
GGA + U	4.20	1.69	3.2
Experiment	4.171 ^a	1.64, ^b 1.77, ^c 1.90 ^d	4, ^e 4.3 ^f

^aReference 22.^bReference 23.^cReference 24.^dReference 25.^eReference 26.^fReference 27.

our purposes. The full structure optimization is performed without any cell or symmetry constraint, until the force is less than 0.01 eV Å⁻¹ per ion. A plane-wave energy cutoff of 500 eV and k -point meshes of $5 \times 5 \times 5$ for HSE06 and $6 \times 6 \times 6$ for GGA + U were used. All calculations were carried out using the Vienna *ab initio* simulation package (VASP).²¹

III. RESULTS AND DISCUSSION

NiO adopts a cubic rocksalt structure with space group $Fm\bar{3}m$. The Ni²⁺ ions in NiO have a high spin d^8 ($t_{2g}^6 e_g^2$) electronic configuration. The calculated lattice parameters, Ni magnetic moments, and band gaps of NiO are listed in Table I. Both the HSE06 functional and the generalized gradient approximation (GGA) + U calculations yield good agreement with experimental values apart from the underestimate of the band gap by about 1 eV in GGA + U .

Upon Li doping, the local environment of one of the Ni ions undergoes substantial distortion with four short and two long Ni-O bonds, whereas the environments of the other six Ni stay unaltered as shown in Table II. The magnetic moment of the nickel ion with the distorted environment is also substantially reduced. The Ni-O bond lengths of this distorted Ni are very similar to those reported for Ni³⁺ in LiNiO₂ (which has a Jahn-Teller distortion).^{27,28} Comparing this to the local density of states (DOS) of the undistorted Ni²⁺ ($t_{2g}^6 e_g^2$) in Fig. 1, the extra unoccupied spin-up e_g state in the distorted Ni DOS shows that its electronic configuration should be $t_{2g}^6 e_g^1$ and hence Ni³⁺.

Figure 2 shows the total density of states of pure NiO and Li-doped NiO (LiNi₇O₈), from both HSE06 and GGA + U calculations. In NiO, the valence-band edge states consist of about 50% Ni and 50% oxygen character, consistent with the large Ni d spectral weight at the top of the valence band obtained from both local-density approximation (LDA) + DMFT calculations¹⁶ and also from experiment.³ Upon

hole doping by substituting one Ni with Li, hole states in Li_{0.125}Ni_{0.875}O emerge with three peaks within the NiO band gap. They are clearly associated with the distorted Ni³⁺, as can be seen from the local density of states (LDOS) in Fig. 1.

However, the band gaps are only opened if structural relaxation is allowed (see Fig. 2). This indicates that Jahn-Teller distortion is the key for the emergence of the band gap and a concomitant hole localization on Ni. Although the band gaps narrow to about 1.3 eV (HSE06) and 0.5 eV (GGA + U) in Li_{0.125}Ni_{0.875}O, they are both consistent with the absence of metallic conductivity in the Li _{x} Ni_{1- x} O system. In order to have a direct comparison with existing experimental results, we have attempted to reproduce the oxygen K -edge absorption spectra from our ground-state structures of NiO and Li_{0.125}Ni_{0.875}O, by plotting out the calculated empty oxygen states with a Gaussian smearing width 1 eV. Although the core-hole effect is not accounted for in our calculations, it has been shown that the main characteristics of the oxygen K -edge absorption spectra can still be correctly reproduced without the core-hole in NiO at the DFT + U level.²⁹ Figure 3 shows the calculated spectra for pure NiO and Li_{0.125}Ni_{0.875}O, along with the experimental spectra taken from Ref. 11. The four peaks A–D in the NiO oxygen absorption spectrum agree well with available experimental spectra. Upon Li doping a new peak E appears in the calculated spectra which corresponds to the peak at 528.5 eV in the experimental spectra. When compared to the density of states in Fig. 2, this new peak E is seen to be the contribution from the states that describe the hybridization between O²⁻ and Ni³⁺. As x increases, the concentration of Ni³⁺ increases and consequently, the intensity of this peak increases. In addition to the peak appearing at about 528.5 eV, there is another peak at about 530 eV which was ignored by the original authors but can be clearly seen in the $x = 0.4$ curve as circled. This peak is also seen in oxygen K edge electron-energy-loss spectroscopy³⁰ and was ignored there also. As we can see from Fig. 2, in addition to the oxygen

TABLE II. Ni-O bond lengths and Ni magnetic moments in the optimized LiNi₇O₈ structure.

	HSE06			GGA + U		
	$d_{\text{Ni-O}}$ (Å)	Bader charge (e)	Magnetic moment (μ_B)	$d_{\text{Ni-O}}$ (Å)	Bader charge (e)	Magnetic moment (μ_B)
Ni (undistorted)	2.07–2.09	+1.43	1.65	2.08–2.10	+1.31	1.69
Ni (distorted)	$1.90 \times 4, 2.13 \times 2$	+1.61	0.88	$1.93 \times 4, 2.14 \times 2$	+1.43	1.05

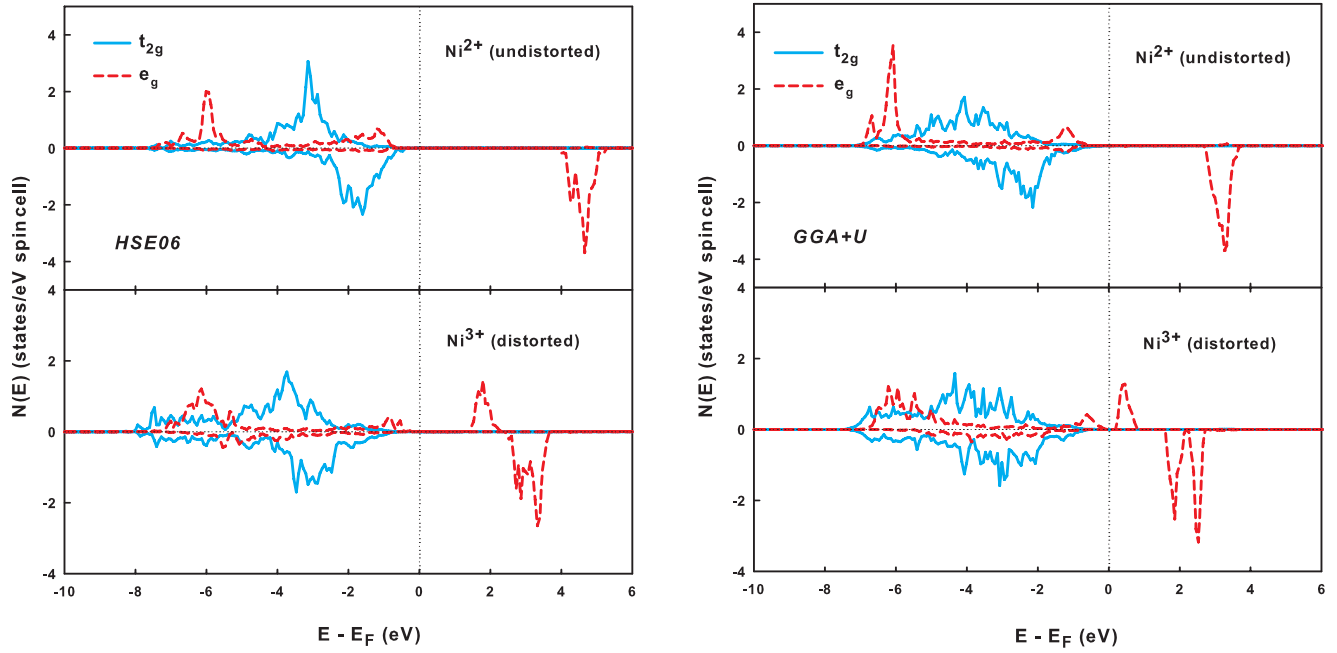


FIG. 1. (Color online) Local density of states of the undistorted and distorted Ni in the optimized LiNi_7O_8 supercell using the HSE06 functional (left) and GGA + U (right).

states associated with peak E, there is also a small oxygen contribution associated with the empty spin-down e_g states of the Ni^{3+} ion. We suggest that these states are the source of the double peak feature at high lithium concentration. To further elucidate where the hole states go in Li-doped NiO, we have plotted out the charge density constructed from the wave functions of the hole states in the band gap, as shown in Fig. 4.

Because HSE06 and GGA + U produce indistinguishable graphs, only the HSE06 case is presented for simplicity. It is clear that hole states mainly reside on one nickel ion with a small amount on the six oxygen ions surrounding the nickel. Again the contribution from oxygen is the consequence of the strong hybridization between the nickel ion and its six surrounding oxygen ions.

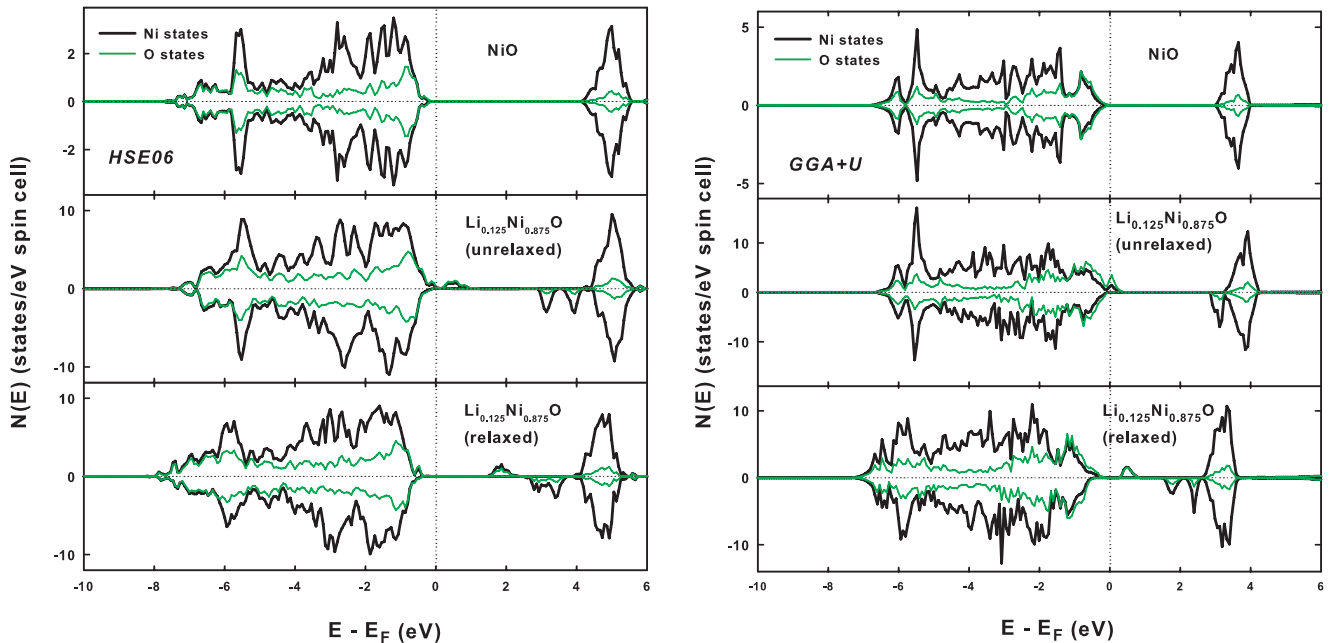


FIG. 2. (Color online) Density of states of NiO and $\text{Li}_{0.125}\text{Ni}_{0.875}\text{O}$ for the HSE06 functional (left) and GGA + U (right) showing both relaxed and unrelaxed cases for $\text{Li}_{0.125}\text{Ni}_{0.875}\text{O}$. Note in the GGA + U density of states for $\text{Li}_{0.125}\text{Ni}_{0.875}\text{O}$, the Ni and O states overlap completely at the spin-up peak around 0.5 eV.

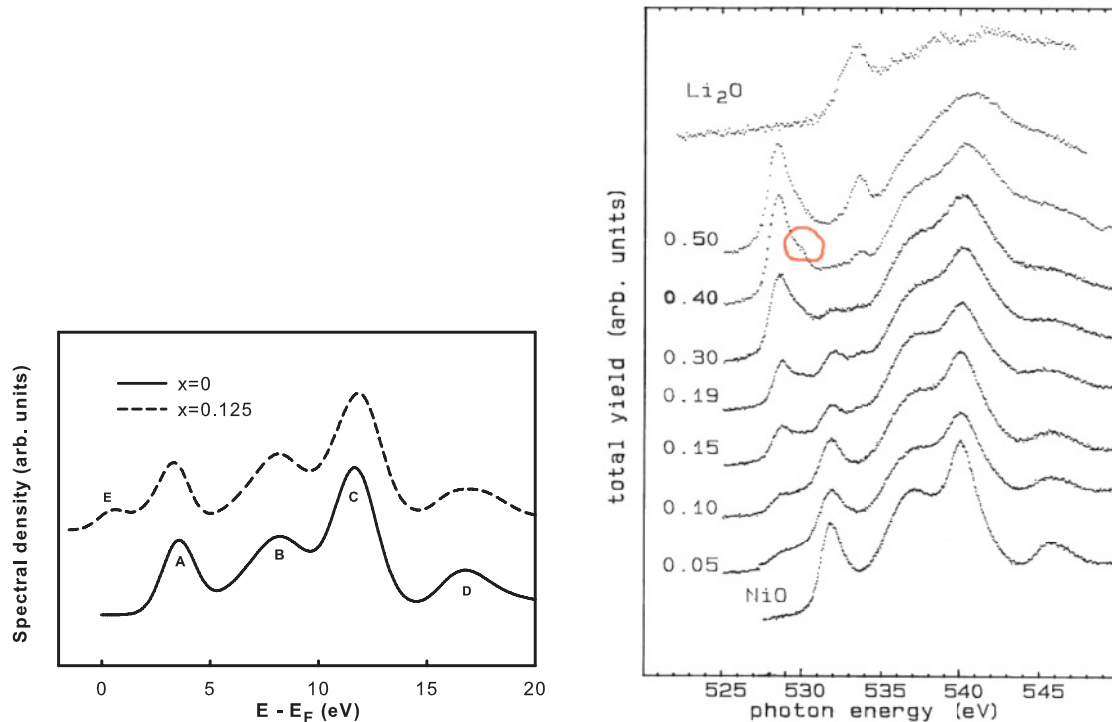


FIG. 3. (Color online) Calculated oxygen empty states (left) of $\text{Li}_x\text{Ni}_{1-x}\text{O}$ with $x = 0, 0.125$ (offset for clarification) using GGA + U compared to experimental result (right) from Ref. 11. Note the peak (circled) in the experimental data for $x = 0.4$.

IV. CONCLUSION

Using full structural optimization, we have calculated the electronic structure of $\text{Li}_{0.125}\text{Ni}_{0.875}\text{O}$ using both the HSE06 and GGA + U approaches. We found that, in spite of the underestimation of the band gap, the DFT + U method with an appropriate value for U produces qualitatively the same results as the HSE06 hybrid functional method. It is demonstrated that the hole induced by lithium doping in NiO predominately

localizes on a Ni ion that is second-neighbor to Li, with some partial density on the surrounding oxide ions. The lithium dopant acts not only as an acceptor, but the relaxation of lithium ions also amplifies the Jahn-Teller distortion around the Ni^{3+} ion, which then functions as a carrier trap. This shows the necessity of including the effect of the lithium ion explicitly. Unlike excitation, where the short lifetime does not allow the lattice time to respond, the physical hole doping is often coupled with lattice distortion and results in the formation of a small polaron. It is therefore not sufficient simply to consider the number of holes that are present at a given level of lithium doping in an otherwise perfect NiO lattice. The oxygen contribution to the hole states is a consequence of a strong hybridization between the Ni 3d and O 2p orbitals, which results in the appearance of the new peak in oxygen absorption spectra. The Ni is hence best described as oxidized from 2+ to 3+ and a strong Jahn-Teller distortion is found as expected. Although a different conclusion on the location of the hole is reached to previous work, our calculated results are still entirely consistent with all previous experiments.

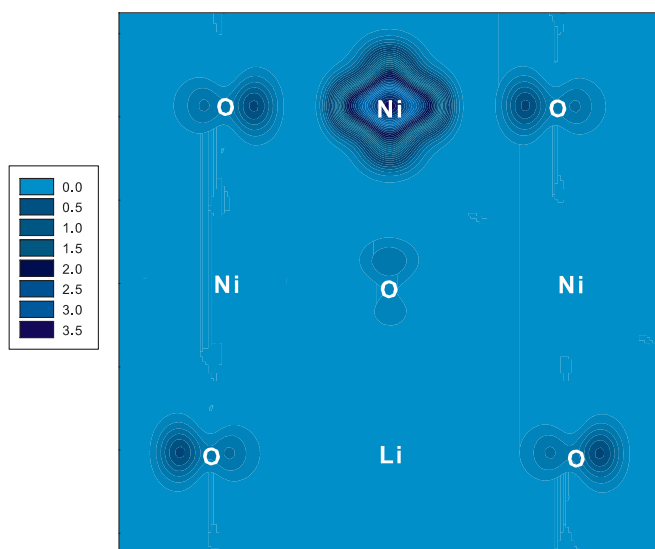


FIG. 4. (Color online) Charge-density contour map ($e/\text{\AA}^3$) of hole states in the (100) plane for $\text{Li}_{0.125}\text{Ni}_{0.875}\text{O}$. Results shown for the HSE06 functional; those for the GGA + U method are indistinguishable.

ACKNOWLEDGMENTS

We thank the Engineering and Physical Sciences Research Council (EPSRC) for funding under Grant No. EP/G005001/1. Via our membership of the U.K.'s HPC Materials Chemistry Consortium, which is funded by EPSRC (EP/F067496), this work made use of the facilities of HECToR, the U.K.'s national high-performance computing service, which is provided by UoE HPCx Ltd. at the University of Edinburgh, Cray Inc., and NAG Ltd., and funded by the Office of Science and Technology through EPSRC's High End Computing Programme.

- ¹J. Zaanen, G. A. Sawatzky, and J. W. Allen, *Phys. Rev. Lett.* **55**, 418 (1985).
- ²T. M. Schuler, D. L. Ederer, S. Itza-Ortiz, G. T. Woods, T. A. Callcott, and J. C. Woicik, *Phys. Rev. B* **71**, 115113 (2005).
- ³G. A. Sawatzky and J. W. Allen, *Phys. Rev. Lett.* **53**, 2339 (1984).
- ⁴A. Fujimori and F. Minami, *Phys. Rev. B* **30**, 957 (1984).
- ⁵Z. Szotek, W. M. Temmerman, and H. Winter, *Phys. Rev. B* **47**, 4029 (1993).
- ⁶S. Massidda, A. Continenza, M. Posternak, and A. Baldereschi, *Phys. Rev. B* **55**, 13494 (1997).
- ⁷A. Ermete, *Mater. Chem. Phys.* **82**, 937 (2003).
- ⁸J. B. Goodenough, D. G. Wickham, and W. J. Croft, *J. Phys. Chem. Solids* **5**, 107 (1958).
- ⁹F. Reynaud, D. Mertz, F. Celestini, J. M. Debierre, A. M. Ghorayeb, P. Simon, A. Stepanov, J. Voiron, and C. Delmas, *Phys. Rev. Lett.* **86**, 3638 (2001).
- ¹⁰I. J. Pickering, G. N. George, J. T. Lewandowski, and A. J. Jacobson, *J. Am. Chem. Soc.* **115**, 4137 (1993).
- ¹¹P. Kuiper, G. Kruizinga, J. Ghijsen, G. A. Sawatzky, and H. Verweij, *Phys. Rev. Lett.* **62**, 221 (1989).
- ¹²W. C. Mackrodt, N. M. Harrison, V. R. Saunders, N. L. Allan, and M. D. Towler, *Chem. Phys. Lett.* **250**, 66 (1996).
- ¹³W. C. Mackrodt and D. S. Middlemiss, *J. Phys.: Condens. Matter* **16**, S2811 (2004).
- ¹⁴I. P. R. Moreira, F. Illas, and R. L. Martin, *Phys. Rev. B* **65**, 155102 (2002).
- ¹⁵F. Tran, P. Blaha, K. Schwarz, and P. Novak, *Phys. Rev. B* **74**, 155108 (2006).
- ¹⁶J. Kunes, V. I. Anisimov, A. V. Lukoyanov, and D. Vollhardt, *Phys. Rev. B* **75**, 165115 (2007).
- ¹⁷P. E. Blochl, *Phys. Rev. B* **50**, 17953 (1994).
- ¹⁸V. K. Aliaksandr, A. V. Oleg, F. I. Artur, and E. S. Gustavo, *J. Chem. Phys.* **125**, 224106 (2006).
- ¹⁹S. L. Dudarev, G. A. Botton, S. Y. Savrasov, C. J. Humphreys, and A. P. Sutton, *Phys. Rev. B* **57**, 1505 (1998).
- ²⁰A. Rohrbach, J. Hafner, and G. Kresse, *Phys. Rev. B* **69**, 075413 (2004).
- ²¹G. Kresse and J. Furthmuller, *Phys. Rev. B* **54**, 11169 (1996).
- ²²L. C. Bartel and B. Morosin, *Phys. Rev. B* **3**, 1039 (1971).
- ²³H. A. Alperin, *J. Phys. Soc. Jpn. Suppl.* **17**, 12 (1962).
- ²⁴B. E. F. Fender, A. J. Jacobson, and F. A. Wedgwood, *J. Chem. Phys.* **48**, 990 (1968).
- ²⁵A. K. Cheetham and D. A. O. Hope, *Phys. Rev. B* **27**, 6964 (1983).
- ²⁶S. Hüfner, J. Osterwalder, T. Riesterer, and F. Hulliger, *Solid State Commun.* **52**, 793 (1984).
- ²⁷H. Chen, C. L. Freeman, and J. H. Harding, *Phys. Rev. B* **84**, 085108 (2011).
- ²⁸A. Rougier, C. Delmas, and A. V. Chadwick, *Solid State Commun.* **94**, 123 (1995).
- ²⁹L. V. Dobysheva, P. L. Potapov, and D. Schryvers, *Phys. Rev. B* **69**, 184404 (2004).
- ³⁰F. Reinert, P. Steiner, S. Hüfner, H. Schmitt, J. Fink, M. Knupfer, P. Sandl, and E. Bertel, *Z. Phys. B: Condens. Matter* **97**, 83 (1995).